

Mercury(II)-stimulated oxidase mimetic activity of silver nanoparticles as a sensitive and selective mercury(II) sensor†

Cite this: *RSC Adv.*, 2014, 4, 5867Guang-Li Wang,^{*a} Xiu-Fang Xu,^a Li-Hua Cao,^b Chong-Hui He,^b Zai-Jun Li^a and Chi Zhang^a

Research on oxidase mimics is challenging but important. In this article, mercury(II) ion enabled citrate-capped silver nanoparticles (Cit-AgNPs) exhibit catalytic activity toward the oxidation of typical chromogenic substrate 3,3',5,5'-tetramethylbenzidine (TMB) by dissolved oxygen under mild conditions, suggesting a new type of oxidase mimic. In addition, the oxidase-like activity of Cit-AgNPs was sensitive to the concentration of mercury(II) ions and selective towards mercury(II) ions among other metal ions. Based on this, a facile colorimetric mercury(II) ion sensor was developed. Hg²⁺ was reduced on the surface of Cit-AgNPs to form Hg-Ag alloys. The Hg-Ag alloys activated oxygen and generated superoxide anions, which oxidized TMB. This discovery indicates the potential of nanoparticles for efficient enzyme mimetics.

Received 19th September 2013
Accepted 5th November 2013

DOI: 10.1039/c3ra45226c

www.rsc.org/advances

1. Introduction

It was well known that natural enzymes have been found extensive applications in various fields because they can catalyze chemical reactions specifically and efficiently under mild conditions. Unfortunately, the catalytic activity of natural enzymes is sensitive to environmental conditions and they can easily be denatured and digested. Furthermore, the preparation, purification and storage of natural enzymes are usually time-consuming and expensive. Therefore, artificial enzyme mimics are of great interest. Enzyme mimics show similar catalytic activities (for example, to oxidize typical substrates to their corresponding oxidation products) as that of natural enzymes and the catalytic reaction process follows typical Michaelis-Menten curves. Since the pioneering work of Yan *et al.*¹ using Fe₃O₄ nanocrystals as peroxidase-mimics, different nanostructures including graphene oxide,² single-wall carbon nanotubes,³ CoFe₂O₄,⁴ FeTe,⁵ metal oxides^{6,7} and bimetallic nanostructures⁸ have also been found to possess peroxidase-like activity which can catalyze the oxidation of typical chromogenic substrates by H₂O₂. It was found that the enzyme-like activity of nanomaterials was dependant on their structure, which could be controlled by the synthesis conditions. In comparison with natural enzymes, enzyme mimics based on nanostructures

possess several advantages including controlled synthesis at a low-cost, high catalytic activity, and high stability under harsh conditions. Therefore, nanomaterials are promising candidates as enzyme mimics.

Oxidation reactions are of fundamental importance in nature. In addition, catalytic oxidations that use oxygen as a green oxidant in organic synthesis are of high significance.⁹ Therefore, research on oxidase mimics is challenging but important. Compared to peroxides mimics, there is less research on oxidase mimics based on nanomaterials. In 2008, Asati *et al.*¹⁰ found that CeO₂ nanoparticles possessed oxidase-like activity. However, it was found that instead of being an oxidase mimic, nanoceria is a plain nanoparticulate oxidant and dissolves completely after the redox reaction.¹¹ Inspired by the fact that Pt is the dominant anode catalyst in fuel cells for the reduction of oxygen to water, Pt-based bimetallic nanostructures including AuPt¹² and PdPt supported on gold nanorods¹³ were explored as oxidase mimics of horseradish peroxidase (HRP) to catalyze the reaction of the substrates *o*-phenylenediamine (OPD) and 3,3',5,5'-tetramethylbenzidine (TMB) in the presence of molecular oxygen. These reports are interesting in the development of novel oxidase mimetic nanomaterials. The oxidase-like activity of the Pt-based nanostructures was obviously inhibited by some metal ions such as iron(II) ions, copper(II) ions and mercuric(II) ions.¹²

In contrast to the idea that the mercuric(II) ions could inhibit the oxidase-like catalytic activity of Au@Pt nanorods,¹² in this contribution, a new kind of mercury(II)-stimulated oxidase mimetic activity of citrate-capped silver nanoparticles (Cit-AgNPs) was found. The reduction of Hg²⁺ on the surface of Cit-AgNPs resulted in the formation of a Hg-Ag alloy, which

^aThe Key Laboratory of Food Colloids and Biotechnology, Ministry of Education, School of Chemical and Material Engineering, Jiangnan University, Wuxi 214122, P. R. China. E-mail: glwang@jiangnan.edu.cn; Fax: +86 510 85917763; Tel: +86 510 85917090

^bNanjing Entry-Exit Inspection and Quarantine Bureau, Nanjing 211106, P. R. China

† Electronic supplementary information (ESI) available. See DOI: 10.1039/c3ra45226c

demonstrated high catalytic effect for typical chromogenic substrates, such as 3,3',5,5'-tetramethylbenzidine (TMB), in the presence of dissolved oxygen. The oxidase-like activity of mercury(II)-stimulated Cit-AgNPs could result in the oxidation of TMB very quickly (within two minutes). The oxidase-like activity of Cit-AgNPs in the presence of Hg^{2+} was highly selective among other metal ions. Therefore, the system could selectively detect Hg^{2+} . This is the first report of oxidase mimics based on non Pt-based nanostructures. In addition, compared to peroxidase, oxidase mimetics could oxidize substrates using oxygen as a green oxidant, which can avoid the use of the destructive and unstable H_2O_2 . Our work is not only helpful to develop efficient nanomaterial-based oxidase mimetics, but also to find new applications of nanomaterial-based catalysts.

2. Experimental

2.1. Chemicals and materials

Silver nitrate, trisodium citrate dihydrate ($\text{Na}_3\text{C}_6\text{H}_5\text{O}_7 \cdot 2\text{H}_2\text{O}$), sodium borohydride (NaBH_4 , 96%), *t*-butanol, *p*-benzoquinone, 3,3',5,5'-tetramethylbenzidine (TMB), AgNO_3 and HgSO_4 were all obtained from Sinopharm Chemical Reagent Co., Ltd (Shanghai, China). All other chemicals used were of analytical grade. All solutions were prepared with ultrapure water ($18.2 \text{ M}\Omega \text{ cm}^{-1}$) obtained from a Healforce water purification system.

2.2. Instrumentation

High resolution transmission electron microscopy (HRTEM) images of Cit-AgNPs were obtained on a JEOL JEM-2100 transmission electron microscope (Hitachi, Japan). The zeta potential and size distribution of the Cit-AgNPs were measured using a ZetaPALS zeta potential and particle size analyzer (Brookhaven, USA). UV-Vis absorption spectroscopic measurements were carried out using a TU-1901 spectrophotometer (Beijing Purkinje General Instrument Co., Ltd, China). Cyclic voltammetry was performed with a CHI 800C electrochemical workstation (Shanghai, China). A conventional three-electrode cell was used, including a Pt wire counter electrode, and a saturated Ag/AgCl reference electrode. An indium tin oxide (ITO) electrode was used as the working electrode. The pH of the HAc-NaAc buffer solution was measured with a glass electrode connected to a PHS-3C pH meter (Shanghai, China).

2.3. Preparation of citrate-capped AgNPs

Citrate-capped AgNPs (Cit-AgNPs) were prepared using a previously reported method¹⁴ with modifications. First, 5 mL $1.0 \times 10^{-2} \text{ mol L}^{-1}$ trisodium citrate and 20 mL $1.0 \times 10^{-3} \text{ mol L}^{-1}$ AgNO_3 were mixed in a 100 mL beaker. Then, 50 mL H_2O was added to the beaker, and 10 mL $2.7 \times 10^{-3} \text{ mol L}^{-1}$ NaBH_4 was added drop by drop with stirring. In this method, the sodium borohydride was a reducing agent capable of reducing Ag^+ to Ag^0 and forming AgNPs in the presence of trisodium citrate as a stabilizing agent. This was a very fast process at room temperature. The colorless reactant mixture immediately turned to dark yellow after about five drops of NaBH_4 had been added,

and then the solution become golden yellow after several drops, which was considered to be indication of the presence of isolated colloidal AgNPs. Then the mixture was allowed to react at ambient temperature for 48 h before further applications.

2.4. Hg^{2+} stimulated oxidase-like activity of Cit-AgNPs for the detection of Hg^{2+}

First, 500 μL Cit-AgNPs, different amounts of HgSO_4 and 300 μL $5.0 \times 10^{-3} \text{ mol L}^{-1}$ TMB were sequentially added to a 5 mL calibrated test tube. Then, 1 mL acetate buffer (HAc-NaAc, pH = 4.0) was added to the above solution. Finally, the mixed solution was dissolved to the required volume with ultrapure water.

3. Results and discussion

The Cit-AgNPs were prepared from AgNO_3 by reductive treatment with NaBH_4 . The HRTEM image revealed the spherical shape of the Cit-AgNPs with an average diameter of about 7–11 nm (Fig. 1A). The hydrodynamic size and zeta potential of the Cit-AgNPs were 30.9 nm and -33.2 mV , respectively, measured by dynamic light scattering measurements. The negative charges of Cit on the surface of the AgNPs resulted in an electrostatic double layer, which provided a repulsive force between separated AgNPs and enabled the Cit-AgNPs to be dispersed stably in an aqueous solution.¹⁵ The final Cit-AgNPs suspension showed a typical intense absorption peak (around 400 nm) (Fig. 1B) due to the surface plasmon excitation.¹⁶

It was found that neither Cit-AgNPs or Hg^{2+} alone showed any catalytic oxidation effect for typical chromogenic substrates such as 3,3',5,5'-tetramethylbenzidine (TMB), in the presence of dissolved oxygen under ambient conditions (Fig. 2 curve a and b). After the addition of Hg^{2+} , the catalytic activity of the Cit-AgNPs was stimulated immediately with the appearance of the characteristic absorbance peaks of the oxidized TMB (oxTMB) at 370 nm and 652 nm and the simultaneous appearance of a bright blue color of the oxTMB (Fig. 2 curve c). In addition, the Cit-AgNPs- Hg^{2+} could also oxidize two other typical substrates such as *o*-phenylenediamine (OPD) and 2,2-azinobis-(3-ethylbenzothiazoline-6-sulfonic acid) (ABTS) to produce their corresponding oxidation products with typical colors. However, the maximum absorption peaks of oxOPD and oxABTS were 450 nm and 417 nm, respectively, which overlapped with the peak of the

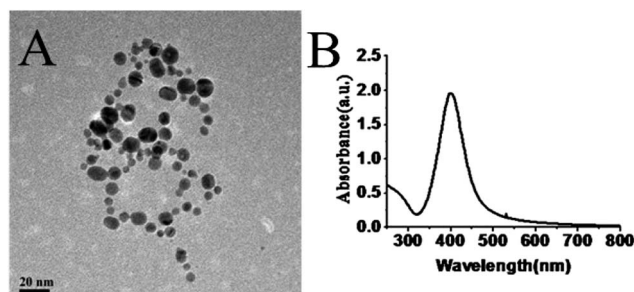


Fig. 1 HRTEM image (A) and UV-vis absorption spectrum (B) of Cit-AgNPs.

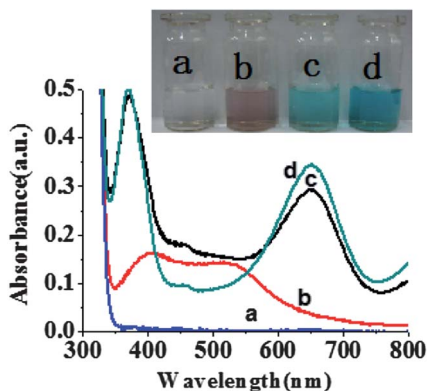
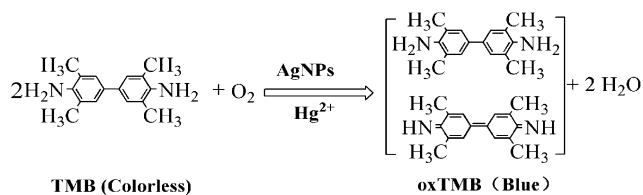


Fig. 2 UV-vis spectra of (a) Hg^{2+} + TMB; (b) Cit-AgNPs + TMB; (c) Cit-AgNPs + Hg^{2+} + TMB; (d) the mixture of Cit-AgNPs and Hg^{2+} was added $500 \mu\text{L } 10^{-2} \text{ mol L}^{-1} \text{ NaBH}_4$ and was allowed to react for 24 h, and finally TMB solution was added. The inset image shows the corresponding colors of the above solutions. All the above solutions were prepared in acetic buffer with pH 4.0.



Scheme 1 The corresponding reaction equation of the oxidation of TMB by dissolved oxygen using Cit-AgNPs and Hg^{2+} .

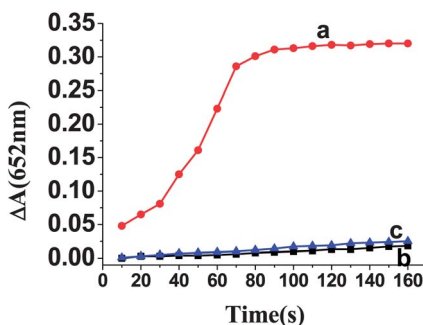


Fig. 3 Time dependent absorbance evolution at 652 nm of the TMB oxidation system (a) Cit-AgNPs + Hg^{2+} + TMB; (b) Hg^{2+} + TMB; (c) Cit-AgNPs + TMB.

AgNPs. Therefore, we chose TMB as a typical substrate to investigate the enzyme-like activity. The oxidase-like activity of Hg^{2+} stimulated Cit-AgNPs for the oxidation of typical organic substrates (TMB) can be described by the equation in Scheme 1. It should be emphasized that the catalytic course of the reaction system was very fast (within 2 min) when using TMB as the model substrate (Fig. 3), though Hg^{2+} or Cit-AgNPs alone hardly showed any catalytic effect at the same time intervals. It was found that the catalytic reaction activity of TMB oxidation by the Cit-AgNPs in the presence of Hg^{2+} decreased obviously after bubbling the solution with high purity nitrogen (Fig. 4),

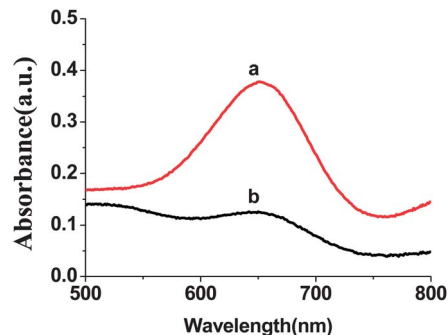


Fig. 4 TMB oxidation was conducted in air with dissolved oxygen (a) and after bubbling the solution with high purity nitrogen for two hours (b).

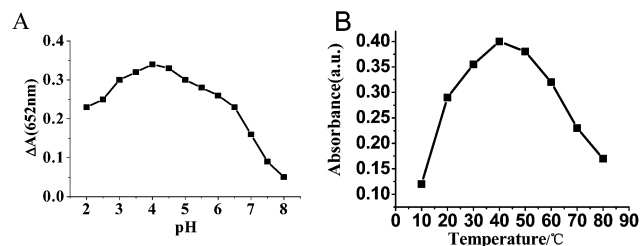


Fig. 5 The catalytic activity of Hg^{2+} stimulated oxidase-like activity of Cit-AgNPs is pH (A) and temperature (B) dependent.

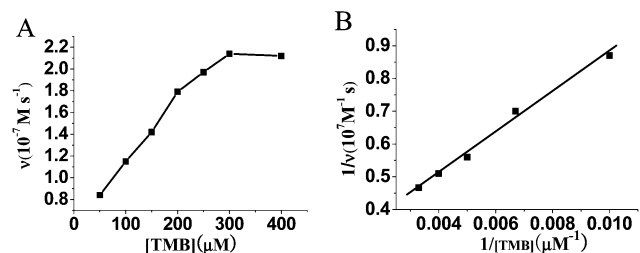


Fig. 6 Michaelis-Menten curve fit (A) and Lineweaver-Burk plot of the double reciprocal of the Michaelis-Menten equation (B).

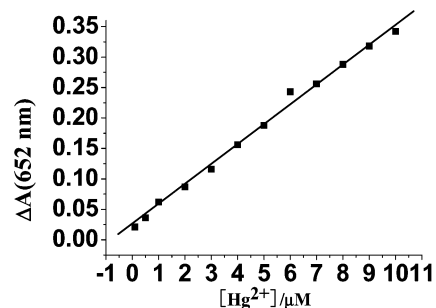


Fig. 7 Linear calibration plot for Hg^{2+} detection.

indicating the nature of the oxidase-like activity of AgNPs- Hg^{2+} using oxygen as a green oxidant. That is, the TMB oxidation originated from the catalytic ability of the catalyst to activate

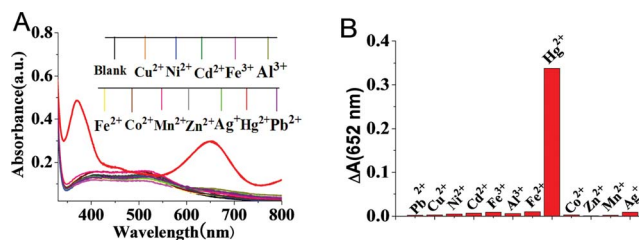


Fig. 8 (A) Catalytic activity of Cit-AgNPs for TMB stimulated by various metal ions; (B) absorption change of TMB at $\lambda = 652$ nm in the presence of Cit-AgNPs and various metal ions. All the metal ions are at concentrations of 1.0×10^{-5} mol L $^{-1}$.

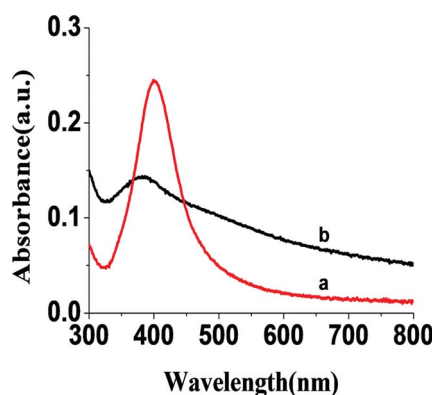
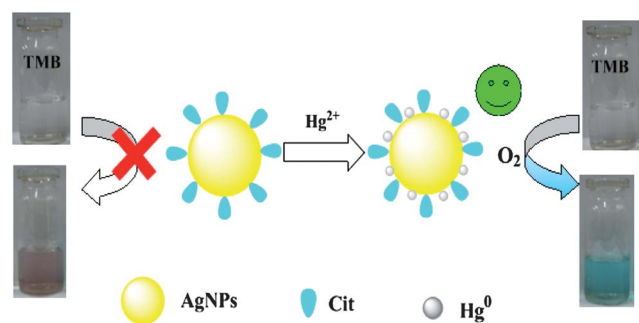


Fig. 9 UV-vis spectra of (a) Cit-AgNPs, and (b) Cit-AgNPs + Hg $^{2+}$ at pH = 4.0.



Scheme 2 The mercury(0) stimulated oxidase-like activity of Cit-AgNPs. Hg $^{2+}$ ions are reduced by citrate and form the Ag-Hg alloy, changing the surface properties of the AgNPs and stimulating the AgNPs-based catalytic oxidation of TMB with dissolved oxygen.

dissolved oxygen but not the direct reaction between Cit-AgNPs or Hg $^{2+}$ with TMB.

Similar to natural enzymes, the catalytic activity of the Cit-AgNPs-Hg $^{2+}$ system was dependent on pH and temperature. The experimental results indicated that the optimized pH and temperature for the proposed system were 4.0 and 40 °C (Fig. 5). It should be pointed out that the Cit-AgNPs showed improved stability compared to HRP at lower/higher pH solutions and at higher temperatures (Fig. S1 †), indicating that Cit-AgNPs as enzyme mimics showed better stability under harsh conditions.

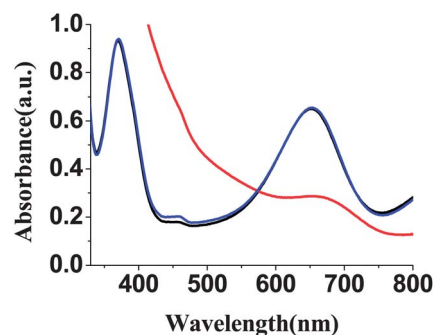


Fig. 10 Oxidation of TMB over the Ag-Hg alloy under different conditions: no scavenger (black line), 10 mM *t*-butanol (blue line), and 5 mol L $^{-1}$ *p*-benzoquinone (red line).

Additionally, the concentration of TMB is a key factor because it determined the absorbance and color level of the reaction system. Therefore, the influence of the concentration of TMB was investigated from 50 to 400 μ M. For all the concentrations investigated, the Cit-AgNPs-Hg $^{2+}$ system could catalyze TMB oxidation in two minutes (Fig. S2 †). The absorption intensity of oxTMB (652 nm) increased gradually with TMB concentration at lower levels until reaching a maximum at high concentrations (about 300 μ M, Fig. S3 †).

Under the optimum conditions, the steady-state kinetics for the catalytic activity of Hg $^{2+}$ stimulated Cit-AgNPs towards the oxidation of TMB with dissolved oxygen were determined and typical Michaelis-Menten curves were obtained (Fig. 6A). The Michaelis-Menten constant (K_m), which is an indicator of enzyme affinity for its substrate, was obtained by using a Lineweaver-Burk plot: $\frac{1}{\nu} = \frac{K_m}{\nu_{max}} \times \frac{1}{[S]} + \frac{1}{\nu_{max}}$, where ν , ν_{max} , $[S]$, and K_m are the reaction rate, maximum reaction velocity, concentration of the substrate, and Michaelis constant, respectively. For the TMB oxidation, K_m is 230 μ M, and ν_{max} is 380 nM s $^{-1}$. The much lower apparent K_m and higher maximum reaction velocity of this system demonstrated that Hg $^{2+}$ stimulated Cit-AgNPs had much higher intrinsic catalytic activity towards oxygen than the natural HRP using H $_2$ O $_2$ as a substrate.^{17,18}

The stimulating effect of Hg $^{2+}$ on the Cit-AgNPs catalytic activity was concentration dependent and could be observed with some sensitivity. With an increasing concentration of Hg $^{2+}$, there was an increase in the absorbance of oxTMB at 652 nm. In fact, under optimal experimental conditions, the calibration curve of the absorbance at 652 nm against Hg $^{2+}$ concentration was linear in a range from 1.0×10^{-7} to 1.0×10^{-5} mol L $^{-1}$ (Fig. 7) with a detection limit of 2.8×10^{-8} mol L $^{-1}$ ($S/N = 3$). The detection limit was lower than the maximum mercury level defined for drinking water by the World Health Organization (WHO) (~ 30 nmol L $^{-1}$).¹⁹ This approach holds great potential for monitoring Hg $^{2+}$ in environmental samples.

It was found that the oxidase-like catalytic effect of Cit-AgNPs was stimulated by Hg $^{2+}$ selectively (Fig. 8). Other metal ions including Pb $^{2+}$, Cu $^{2+}$, Ni $^{2+}$, Cd $^{2+}$, Fe $^{3+}$, Al $^{3+}$, Fe $^{2+}$, Co $^{2+}$, Zn $^{2+}$, Mn $^{2+}$ and Ag $^+$ did not display the same stimulating catalytic

effects for TMB oxidation and no absorption at 652 nm of oxTMB could be distinguished owing to the catalysis of Cit-AgNPs in the presence of other metal ions even at a concentration of $1.0 \times 10^{-5} \text{ mol L}^{-1}$.

It was found that citrate-capped noble metal nanoparticles could reduce Hg^{2+} to elemental mercury (Hg^0).²⁰ A slight blue shift in the absorption peak from 400 to 397 nm was observed after the addition of Hg^{2+} to Cit-AgNPs (Fig. 9). This phenomenon may be ascribed to the reduction of Hg^{2+} by Cit-AgNPs and subsequent deposition of elemental Hg on the surface of AgNPs, yielding the Ag-Hg alloy due to the high affinity between Ag and Hg.^{21,22} In order to confirm that Hg^0 results in the enhancement of the catalytic activity of AgNPs, Ag-Hg alloy^{23,24} synthesized by NaBH_4 (a stronger reductant than citrate) reduction of Hg^{2+} was used for TMB oxidation. The Ag-Hg alloy obtained by NaBH_4 reduction showed even higher oxidase-like catalytic activity for TMB oxidation than that obtained by Cit-AgNPs reduction of Hg^{2+} (Fig. 2 curve c and d). Because NaBH_4 reduces Hg^{2+} to Hg^0 more easily than sodium citrate, much more Hg^0 was produced on the surface of the AgNPs. As a result, a much more enhanced catalytic activity was observed. In addition, cyclic voltammogram measurements of the Cit-AgNPs, the mixture of Hg^{2+} and Cit-AgNPs, and the mixture of Cit-AgNPs, Hg^{2+} and NaBH_4 indicated that there was a new oxidation peak for the mixture of Hg^{2+} and Cit-AgNPs, and Cit-AgNPs, Hg^{2+} and NaBH_4 besides the oxidation peak of Ag (around 0.4 V, Fig. S4[†]). The new oxidation peak at around 0.2 V might be attributed to the oxidation of elemental Hg. These cyclic voltammogram measurements provided evidence for the formation of elemental Hg (Hg^0) in our experiment.

Control experiments confirmed that a mixture of Hg^{2+} and sodium citrate or a mixture of Hg^{2+} and NaBH_4 did not catalyze the oxidation of TMB with dissolved oxygen. In conclusion, the capping agent, sodium citrate, on the surface of the AgNPs acted as a reducing reagent to reduce Hg^{2+} to Hg^0 . Hg^0 was easily deposited on the surface of AgNPs to form the Ag-Hg alloy due to the high affinity between Ag and Hg^{2+} ,²² and changed the surface properties of the AgNPs, stimulating their oxidase-like activity. The mechanism for Hg^{2+} detection is depicted in Scheme 2.

To elucidate the main reactive species responsible for the oxidation of TMB over the Ag-Hg alloy, different quenchers were employed to scavenge the relevant reactive species.^{25,26} Here, *t*-butanol had no influence on the oxidation of TMB, indicating that no $\cdot\text{OH}$ existed in the solution. In contrast, the introduction of *p*-benzoquinone significantly restrains the oxidation of TMB, suggesting that the superoxide anion ($\text{O}_2^{\cdot-}$) plays a key role in the oxidation of TMB (Fig 10). Our findings were in accordance with the recent report that some metal NPs could activate molecular oxygen to generate $\text{O}_2^{\cdot-}$.²⁷ In our experiment, the Ag-Hg alloy activated molecular oxygen to generate $\text{O}_2^{\cdot-}$ and contributed to the catalytic activity for TMB oxidation.

4. Conclusion

In conclusion, $\text{Hg}(\text{II})$ can stimulate the oxidase-like activity of Cit-AgNPs selectively and sensitively, which enables a facile and

fast colorimetric assay for Hg^{2+} . Owing to the facile preparation of AgNPs and their potential for the chemical reaction activity, our work could help to develop a variety of applications of oxidase-based, simple, cost-effective, and easy-to-make sensors in biotechnology, medicine and environmental chemistry.

Acknowledgements

This work was supported by the National Natural Science Foundation of China (no. 21275065, 21005031), the Fundamental Research Funds for the Central Universities (JUSRP51314B), the 111 Project (B13025) and Project of Jiangsu Inspection and Quarantine Bureau (2011KJ17).

References

- 1 L. Gao, J. Zhuang, L. Nie, J. Zhang, Y. Zhang, N. Gu, T. Wang, J. Feng, D. L. Yang, S. Perrett and X. Y. Yan, *Nat. Nanotechnol.*, 2007, **2**, 577–583.
- 2 Y. Song, K. Qu, C. Zhao, J. Ren and X. Qu, *Adv. Mater.*, 2010, **22**, 2206–2210.
- 3 Y. Song, X. Wang, C. Zhao, K. Qu, J. Ren and X. Qu, *Chem.–Eur. J.*, 2010, **16**, 3617–3621.
- 4 W. B. Shi, X. D. Zhang, S. H. He and Y. M. Huang, *Chem. Commun.*, 2011, **47**, 10785–10787.
- 5 R. Prathik, Z. H. Lin, C. T. Liang and H. T. Chang, *Chem. Commun.*, 2012, **48**, 4079–4081.
- 6 R. André, F. Natálio, M. Humanes, J. Leppin, K. Heinze, R. Wever, H. C. Schröder, W. E. G. Müller and W. Tremel, *Adv. Funct. Mater.*, 2011, **21**, 501–509.
- 7 J. S. Mu, Y. Wang, M. Zhao and L. Zhang, *Chem. Commun.*, 2012, **48**, 2540–2542.
- 8 W. W. He, X. C. Wu, J. B. Liu, X. N. Hu, K. Zhang, S. Hou, W. Zhou and S. Xie, *Chem. Mater.*, 2010, **22**, 2988–2994.
- 9 T. Punniyamurthy, S. Velusamy and J. Iqbal, *Chem. Rev.*, 2005, **105**, 2329–2363.
- 10 A. Asati, S. Santra, C. Kaittanis, S. Nath and J. M. Perez, *Angew. Chem., Int. Ed.*, 2009, **48**, 2308–2312.
- 11 Y. F. Peng, X. J. Chen, G. S. Yi and Z. Q. Gao, *Chem. Commun.*, 2011, **47**, 2916–2918.
- 12 J. B. Liu, X. N. Hu, S. Hou, T. Wen, W. Q. Liu, X. Zhu and X. C. Wu, *Chem. Commun.*, 2011, **47**, 10981–10983.
- 13 K. Zhang, X. N. Hu, J. B. Liu, J. J. Yin, S. Hou, T. Wen, W. W. He, Y. L. Ji, Y. T. Guo, Q. Wang and X. C. Wu, *Langmuir*, 2011, **27**, 2796–2803.
- 14 R. C. Doty, T. R. Tshikhudo, M. Brust and D. G. Fernig, *Chem. Mater.*, 2005, **17**, 4630–4635.
- 15 M. Moskovits and B. Vlckova, *J. Phys. Chem. B*, 2005, **109**, 14755–14758.
- 16 X. L. Gao, G. H. Gu, Z. S. Hu, Y. Guo, X. Fu and J. M. Song, *Colloids Surf., A*, 2005, **254**, 57–61.
- 17 W. W. He, Y. Liu, J. S. Yuan, J. J. Yin, X. C. Wu, K. Zhang, J. B. Liu, C. Y. Chen, Y. L. Ji and Y. T. Guo, *Biomaterials*, 2011, **32**, 1139–1147.
- 18 J. F. Yin, H. Q. Cao and Y. X. Lu, *J. Mater. Chem.*, 2012, **22**, 527–534.

- 19 World Health Organization, Guidelines for Drinking-Water Quality: Incorporating 1st and 2nd Addenda, Recommendations, 3rd edn, 2008, vol. 1, http://www.who.int/water_sanitation_health/dwq/fulltext.pdf, accessed November 10, 2010.
- 20 C. Y. Lin, C. J. Yu, Y. H. Lin and W. L. Tseng, *Anal. Chem.*, 2010, **82**, 6830–6837.
- 21 A. Henglein and C. Brancewicz, *Chem. Mater.*, 1997, **9**, 2164–2167.
- 22 T. Morris, H. Copel, E. McLinden, S. Wilson and G. Szuowski, *Langmuir*, 2002, **18**, 7261–7264.
- 23 K. P. Lisha and P. T. Anshup, *Gold. Bull.*, 2009, **42**, 144–152.
- 24 M. Rex, F. E. Hernandez and A. D. Campiglia, *Anal. Chem.*, 2006, **78**, 445–451.
- 25 R. F. Dong, B. Z. Tian, C. Y. Zeng, T. Y. Li, T. T. Wang and J. L. Zhang, *J. Phys. Chem. C*, 2013, **117**, 213–220.
- 26 C. H. An, J. Z. Wang, C. Qin, W. Jiang, S. T. Wang, Y. Li and Q. H. Zhang, *J. Mater. Chem.*, 2012, **22**, 13153–13158.
- 27 S. F. Cai, H. P. Rong, X. F. Yu, X. W. Liu, D. S. Wang, W. He and Y. D. Li, *ACS. Catal.*, 2013, **3**, 478–486.